PROPAGATION OF ELECTROMAGNETIC WAVES IN PLANAR BOUNDED PLASMA REGION

E. A. Soliman [†]**, A. Helaly, and A. A. Megahed**

Cairo University
Faculty of Engineering
Department of Engineering Physics and Mathematics
12211 Giza, Egypt

Abstract—This paper aims at developing a technique to calculate the reflection, absorption, and transmission of electromagnetic waves by a bounded plasma region. The model chosen for this study is a magnetized, steady-state, two-dimensional, nonuniform plasma slab, which is presented by a number of parallel flat layers. It is assumed that the electron density is constant in each layer such that the overall electron density profile across the slab follows any prescribed distribution function. The proposed technique is referred to as Scattering Matrix Model (SMM). The fields in each layer are written in the form of summation of the appropriate eigen functions weighted by unknown scattering coefficients. These coefficients are determined via the application of the appropriate boundary conditions at each interface. The effect of varying the wave frequency and the plasma parameters on the reflected, transmitted, and absorbed powers are presented and discussed.

1. INTRODUCTION

In recent years there has been a definite trend toward using plasmas as absorbers or reflectors of the electromagnetic radiation depending on a specified application [1–5]. Such study is very important to find out the suitable parameters of the plasma which affect the reflection, absorption, and transmission of the electromagnetic energy. Studying the electromagnetic waves interaction with a stratified layered media can be carried out using either analytical or numerical methods.

[†] Also with the Department of Electrical and Computer Engineering, College of Engineering, King AbdulAziz University, P.O. Box 80204, Jeddah 21589, Saudi Arabia

Gilbert and Backus [6] handled the problem of elastic wave propagation using what they called propagator matrices. Morgan et al. [7], concerned with the problem of reflection from a media composed of discrete anisotropic layers. They employed a 4×4 transition matrix for each layer which was found explicitly in terms of the solution of an algebraic eigenvalue problem. Titchener and Willis [8] used an alternative approach, they introduced a 2×2 admittance matrix, for which a first-order equation of Ricatti type may be derived. Laroussi and Roth [5] suggested a ray tracing technique to deal with the problem of electromagnetic waves interaction with a nonuniform plasma slab. Their model neglected the multi reflection of the rays inside the slab. Wide band results can be obtained by studying the transient solution for a plane wave incident on a plasma slab. Gray [9] presented transient solution for a plane wave incident on a plasma half-space via Laplace transformation of the frequency domain solution. Zhang and Tschu [10] used a somewhat similar approach involving Fourier transformation of frequency domain results to compute pulse propagation through an anisotropic plasma layer. Lee [11] presented results for pulse distortion for a plane wave propagation through a uniform isotropic plasma. Whitman and Felsen [12] have presented an asymptotic solution for pulse propagation in a stratified isotropic plasma, but their results were limited to large propagation times and distances. Hagelaar et al. [13] investigated the interaction between electromagnetic fields and a hydrogen plasma in a resonance-type microwave plasma reactor, by combining an elementary theoretical analysis and a self-consistent two-dimensional numerical model. Hojo et al. [14] have studied the full-wave simulations on ultrashort-pulse reflectometry for helical plasmas based on the FD-TD method in two dimensions. Kunz and Luebbers [15] have used FD-TD for studying the electromagnetic waves interaction with plasma slab.

Helaly et al. studied the electromagnetic waves scattering by nonuniform magnetized plasma cylinder [16] and nonuniform plasma sphere [17]. They have introduced the Scattering Matrix Model (SMM) and used the Impedance Boundary Conditions (IBC) for formulating these problems. In SMM, they expand the fields in each layer into group of appropriate eigen functions weighted by unknown expansion coefficients. Successive application of the boundary conditions, which require the continuity of the tangential electric and magnetic fields at the interfaces, results in a set of equations which are solved for the unknown expansion coefficients. In IBC, the authors replace the highly conducting plasma object by an impedance surface at which the impedance boundary conditions are applied.

In this paper, the electromagnetic waves interaction with a

nonuniform plasma slab is studied. The nonuniform slab is represented by a number of parallel flat layers. It is assumed that the electron density is constant in each layer such that the overall electron density profile across the slab follows any prescribed distribution function. Scattering Matrix Model (SMM) for this problem is introduced in Section 2. Numerical results showing the effect of the wave frequency on the behavior of the reflected, transmitted, and the absorbed powers are presented in Section 3. The effect of varying the plasma parameters on the degree of reflection, transmission, and absorption are also investigated. Section 4 includes the important conclusions obtained from the numerical results.

2. SCATTERING MATRIX MODEL (SMM)

The plasma slab under consideration is nonuniform, cold, weakly ionized, steady-state, collisional, and magnetized by a static uniform background magnetic field in the y-z plane and making an angle ϕ with the z-axis, as shown in Fig. 1. The nonuniform plasma slab is represented by p flat layers parallel to the y-z plane. Each layer is assumed to have a constant electron density, but the overall electron density profile across the whole slab should follow a prescribed distribution function. The magnetic field of the incident wave is assumed polarized in the +ve z-direction. Its time dependent is $e^{i\omega t}$ and suppressed throughout.
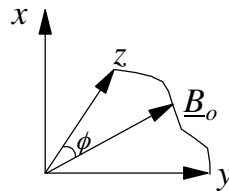

Figure 1. Orientation of the background magnetic field.

The corresponding propagation constant in each plasma layer is given by:

$$\tilde{\gamma} = i\frac{\omega}{c}\tilde{\mu} \qquad (1)$$

where ω is the radial operating frequency, c is the speed of light, and $\tilde{\mu}$ is the complex refractive index of the plasma layer under consideration. The ($\tilde{\ }$) sign over each symbol indicates a complex quantity. Assuming the following conditions [18]: 1) the effect of the plasma on the wave is due to the electrons only, 2) the background magnetic field $\underline{B}_o$ is

uniform, 3) collisions make the plasma medium be lossy, and 4) the force exerted on the moving particles by the magnetic field is negligible compared to that caused by the electric field. This yields an expression for the complex refractive index $\tilde{\mu}$ [19]:

$$\tilde{\mu}^2 =$$

$$1 - \frac{\dfrac{\omega_P^2}{\omega^2}}{\left[1 - i\dfrac{\nu}{\omega} - \dfrac{\dfrac{\omega_{ce}^2}{\omega^2}\sin^2\psi}{2\left(1 - \dfrac{\omega_P^2}{\omega^2} - i\dfrac{\nu}{\omega}\right)}\right] \pm \left[\dfrac{\dfrac{\omega_{ce}^2}{\omega^2}\sin^4\psi}{4\left(1 - \dfrac{\omega_P^2}{\omega^2} - i\dfrac{\nu}{\omega}\right)} + \dfrac{\omega_{ce}^2}{\omega^2}\cos^2\psi\right]^{1/2}} \tag{2}$$

where ω_P is the plasma frequency, ν is the collision frequency, and ω_{ce} is the electron cyclotron frequency, while ψ is the angle between the direction of propagation $\underline{u}_\gamma$ and the background magnetic field. The $\pm$ sign in equation (2) indicates two possible modes of propagation which are referred to as mode #1 and mode #2 corresponding to the +ve and $-$ve signs, respectively [4]. In SMM model, there are two waves assumed to propagate in each layer in ζ_i^+ and ζ_i^- directions, see Fig. 2. Electric and magnetic fields in the ith layer are given by:

$$\underline{H}_i^+ = H_i^+ \exp\left(-\tilde{\gamma}_i\zeta_i^+\right)\underline{u}_z \tag{3a}$$

$$\underline{H}_i^- = H_i^- \exp\left(-\tilde{\gamma}_i\zeta_i^-\right)\underline{u}_z \tag{3b}$$

$$\underline{E}_i^+ = \tilde{\eta}_i H_i^+ \exp\left(-\tilde{\gamma}_i\zeta_i^+\right)\left[-\sin\theta_i\underline{u}_x + \cos\theta_i\underline{u}_y\right] \tag{3c}$$

$$\underline{E}_i^- = \tilde{\eta}_i H_i^- \exp\left(-\tilde{\gamma}_i\zeta_i^-\right)\left[-\sin\theta_i\underline{u}_x - \cos\theta_i\underline{u}_y\right] \tag{3d}$$

where $(\underline{E}_i^+, \underline{E}_i^-)$ and $(\underline{H}_i^+, \underline{H}_i^-)$ are the electric and magnetic field vectors of the waves propagating in ζ_i^+ and ζ_i^- directions, respectively. θ_i is the angle between the wave travelling in the ζ_i^+ direction and the x-axis. $\underline{u}_x, \underline{u}_y$, and $\underline{u}_z$ are unit vectors in the x-, y-, and z-directions, respectively. $\tilde{\eta}_i$ is the wave impedance in the ith plasma layer. H_i^+ and H_i^- are unknown complex scattering coefficients, to be determined via the application of the boundary conditions. Continuity of the tangential field components at the ith interface results in the following:

$$H_{i-1}^+\exp(-\tilde{\gamma}_{i-1}\zeta_i) + H_{i-1}^-\exp(\tilde{\gamma}_{i-1}\zeta_i) = H_i^+\exp(-\tilde{\gamma}_i\zeta_i) + H_i^-\exp(\tilde{\gamma}_i\zeta_i) \tag{4a}$$
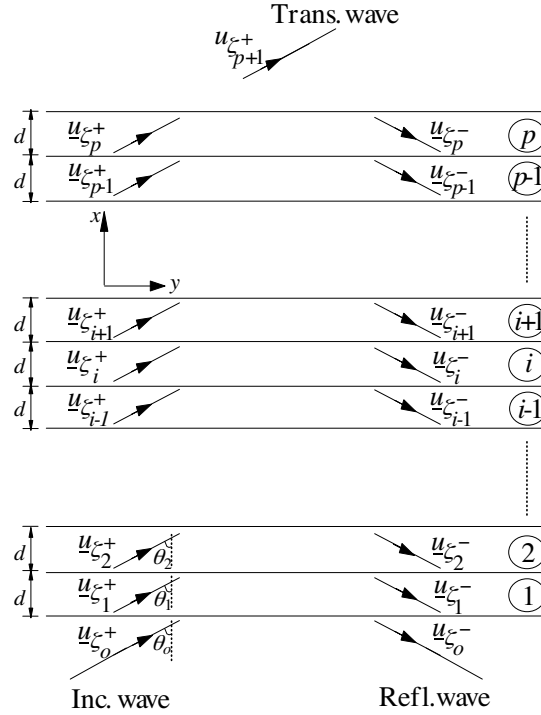
Figure 2. Scattering Matrix Model (SMM).

$$\left[\tilde{\eta}_{i-1} H_{i-1}^+ \exp(-\tilde{\gamma}_{i-1}\zeta_i) \cos\theta_{i-1} - \tilde{\eta}_{i-1} H_{i-1}^- \exp(\tilde{\gamma}_{i-1}\zeta_i) \cos\theta_{i-1} \right]$$
$$= \left[\tilde{\eta}_i H_i^+ \exp(-\tilde{\gamma}_i\zeta_i) \cos\theta_i - \tilde{\eta}_i H_i^- \exp(\tilde{\gamma}_i\zeta_i) \cos\theta_i \right] \quad (4b)$$

where $\zeta_i = (i-1)d/\cos\theta_i$, and d is the layer thickness. Equations (4a) and (4b) can be written in a more compact form as follows:

$$\begin{pmatrix} H_i^+ \\ H_i^- \end{pmatrix} = S_i \cdot \begin{pmatrix} H_{i-1}^+ \\ H_{i-1}^- \end{pmatrix} \quad (5)$$

where S_i is the *scattering matrix* of the ith boundary. It relates the scattering coefficients of the $(i-1)$th and the ith layers, and is given by:

$$S_i = \begin{pmatrix} \exp(-\tilde{\gamma}_i\zeta_i) & \exp(\tilde{\gamma}_i\zeta_i) \\ \tilde{\eta}_i \exp(-\tilde{\gamma}_i\zeta_i) \cos\theta_i & -\tilde{\eta}_i \exp(\tilde{\gamma}_i\zeta_i) \cos\theta_i \end{pmatrix}^{-1}$$

$$\times \begin{pmatrix} \exp(-\tilde{\gamma}_{i-1}\zeta_i) & \exp(\tilde{\gamma}_{i-1}\zeta_i) \\ \tilde{\eta}_{i-1}\exp(-\tilde{\gamma}_{i-1}\zeta_i)\cos\theta_{i-1} & -\tilde{\eta}_{i-1}\exp(\tilde{\gamma}_{i-1}\zeta_i)\cos\theta_{i-1} \end{pmatrix} \quad (6)$$

Successive application of equation (5) beginning with the first interface until the last interface results in the following matrix equation:

$$\begin{pmatrix} H_{p+1}^+ \\ H_{p+1}^- \end{pmatrix} = S_g \cdot \begin{pmatrix} H_0^+ \\ H_0^- \end{pmatrix} \quad (7)$$

where:

$$S_g = \prod_{i=p+1}^{1} S_i \quad (8)$$

The matrix S_g can be referred to as the *global scattering matrix* which gives the relation between the coefficients of the 0th layer (i.e., free space, below the slab, into which the reflected wave is returned) and the $(p+1)$th layer (i.e., free space, above the slab, into which the transmitted wave is propagating). Obviously, the coefficients H_0^+, H_0^-, and H_{p+1}^+ are the complex magnetic field coefficients of the incident (H_i), the reflected (H_r), and the transmitted (H_t), waves, respectively. Since there is no wave reflected in the free space upper region, layer $(p+1)$, the coefficient H_{p+1}^- vanishes. As a consequence, equation (7) can be written in the following form:

$$\begin{pmatrix} H_t \\ 0 \end{pmatrix} = S_g \cdot \begin{pmatrix} H_i \\ H_r \end{pmatrix} \quad (9)$$

From the above matrix equation H_r and H_t can be obtained in terms of H_i as follows:

$$H_r = S_r H_i \quad (10a)$$
$$H_t = S_t H_i \quad (10b)$$

where S_r and S_t are the required complex scattering coefficients. Therefore, the normalized reflected, transmitted, and absorbed powers are, respectively, given by:

$$P_r = |S_r|^2 \quad (11a)$$
$$P_t = |S_t|^2 \quad (11b)$$
$$P_a = 1 - P_r - P_t \quad (11c)$$

3. NUMERICAL RESULTS

The absorbed, transmitted, and reflected powers can be obtained using the Scattering Matrix Model (SMM) described in the previous section. In order to check the model, some tests were performed. Tests included setting the constitutive parameters of the plasma slab equal to those of free space. This results in having a transmitted power equal to the incident one, i.e., both the reflected and absorbed powers vanish, as one would expect.

A second test is done by considering a slab which is identical to the case studied by Kunz et al. [15]. The slab is magnetized by background magnetic field applied in the same direction of the wave propagation. Consequently, the propagating modes in the plasma are: right hand circular polarized (RCP) and left hand circular polarized (LCP) modes. The slab parameters are: $\omega_p = 50\,\text{GHz}$, $\omega_{ce} = 3 \times 10^{11}\,\text{rad/sec}$, $\nu = 2 \times 10^{10}\,\text{rad/sec}$ and the slab thickness is $9\,\text{mm}$.
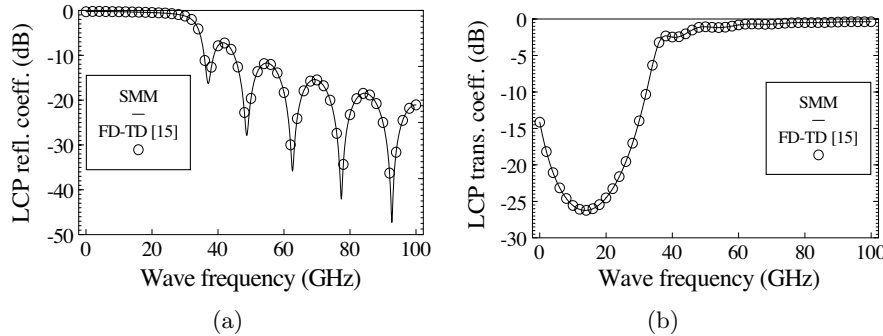

Figure 3. Coefficients of the LCP mode versus wave frequency for plasma slab magnetized by a background magnetic field in the wave propagation direction: $\theta_o = 0°$, $\omega_{ce} = 3 \times 10^{11}\,\text{rad/sec}$, $\nu = 3 \times 10^{11}\,\text{rad/sec}$, $\omega_p = 50\,\text{GHz}$, slab thickness $= 9\,\text{mm}$: (a) reflection, and (b) transmission coefficient.

The reflection and the transmission coefficients computed using SMM as well as the results published in [15] for the LCP and RCP propagation modes are shown in Figs. 3 and 4, respectively. These figures show that the results of the SMM are in very good agreement with those obtained using FD-TD technique [15], which is reported to be a highly time and storage consuming numerical technique. These tests validate the proposed model.

Now, the SMM is applied on a nonuniform plasma slab example. In order to calculate the reflected, transmitted, and absorbed powers,
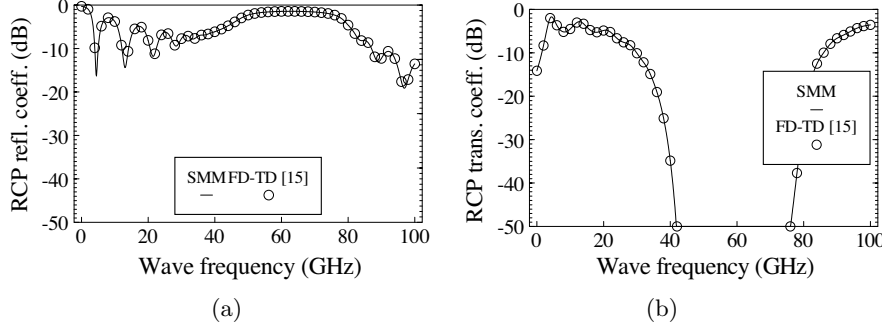
Figure 4. Coefficients of the RCP mode versus wave frequency for plasma slab magnetized by a background magnetic field in the wave propagation direction: $\theta_o = 0°$, $\omega_{ce} = 3 \times 10^{11}$ rad/sec, $\nu = 3 \times 10^{11}$ rad/sec, $\omega_p = 50$ GHz, slab thickness = 9 mm: (a) reflection, and (b) transmission coefficient.

i.e., $P_r, P_t,$ and P_a, of this slab, it is divided into number of flat layers. Electron density is constant in each layer, but the overall density profile can follow any prescribed distribution function. Physically, the distribution function requires maximum density at the center and zero density at the plasma-air interface. The experiments [5] show that the electron density profile for plasma objects may follow a parabolic curve with center density N_o.

The electron cyclotron frequency ω_{ce} is taken to be equal to 4 GHz. The background magnetic field is assumed to lie in the y-z plane and make an angle ϕ with the z-axis. The solution accuracy depends on the number of layers used in the model. Increasing the layers number will increase the solution accuracy. Fig. 5 shows the normalized reflected power versus wave frequency for a slab divided into 10, 20, 30, 40, and 50 layers. The incident plane wave makes an angle $\theta_o = 30°$ with the normal to the slab. Plasma parameters are: $\omega_{ce} = 4$ GHz, $\nu = 10$ MHz, $N_o = 10^{14}$ m^{-3}, and $\phi = 90°$. It is worth noting that those parameters are selected such that only mode #2, near resonance, is greatly affected by the wave frequency in the band of interest. Since we are interested in the behavior of the reflected, transmitted, and absorbed powers versus wave frequency, only mode #2 will be taken into account from now on.

Fig. 5 shows that the numerical values of the reflected power converge to each others for large layer numbers. As a consequence, dividing the slab into 40 layers is proved to be good enough for representing the nonuniform nature of the density profile. All numerical results presented in the rest of this section are computed
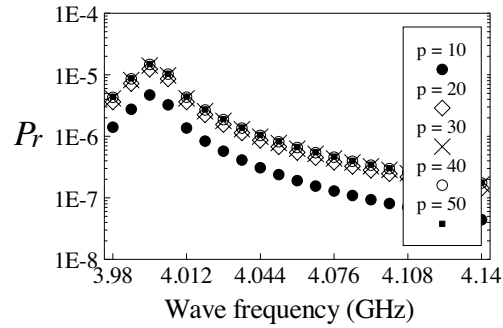
Figure 5. Normalized reflected power versus wave frequency: $\phi = 90°$, $\theta_o = 30°$, $\omega_{ce} = 4\,\text{GHz}$, $\nu = 10\,\text{MHz}$, $N_o = 10^{14}\,\text{m}^{-3}$.
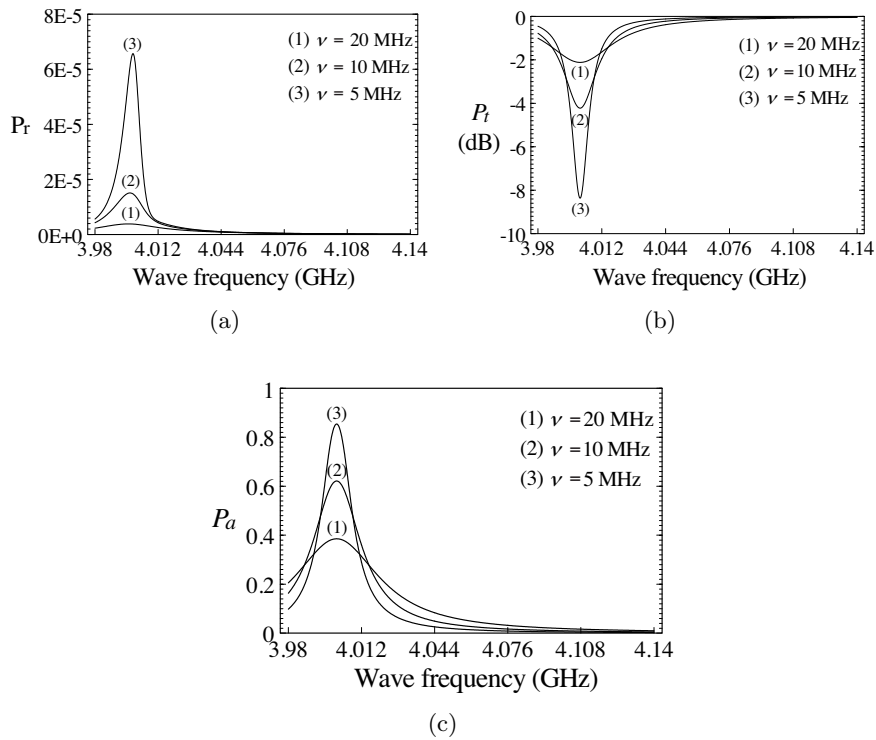

Figure 6. Normalized power versus wave frequency: $\phi = 90°$, $\theta_o = 30°$, $\omega_{ce} = 4\,\text{GHz}$, $N_o = 10^{14}\,\text{m}^{-3}$: (a) reflected, (b) transmitted, and (c) absorbed power.
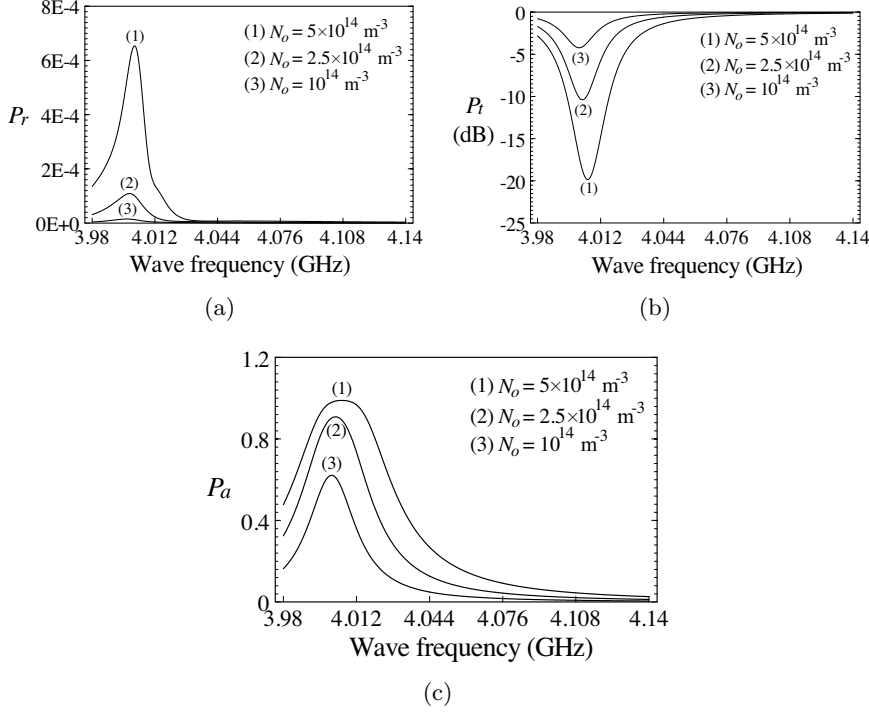
Figure 7. Normalized power versus wave frequency: $\phi = 90°$, $\theta_o = 30°$, $\omega_{ce} = 4\,\text{GHz}$, $\nu = 10\,\text{MHz}$: (a) reflected, (b) transmitted, and (c) absorbed power.

using 40 layers configuration.

For $\theta_o = 30°$, $\phi = 90°$ and for three values of the collision frequency, $\nu = 20\,\text{MHz}$, $10\,\text{MHz}$, and $5\,\text{MHz}$: Figs. 6a, 6b, and 6c show P_r, P_t, and P_a, respectively, versus the wave frequency. Figs. 6a and 6b show that the peak reflected power increases with decreasing the collision frequency, while the minimum transmitted power increases with increasing the collision frequency. Fig. 6c shows that the minimum absorbed power decreases with increasing the collision frequency. This can be explained on the basis that for infrequent collisions, the particles spiral out to large gyroradii where they fall through a large potential difference, and therefore absorb more energy from the wave. Fig. 6 shows that the resonance frequency is almost independent on the collision frequency.

Figs. 7a, 7b, and 7c show , respectively, versus wave frequency for these values of the center density: $N_o = 5 \times 10^{14}\,\text{m}^{-3}$, $N_o = 2.5 \times 10^{14}\,\text{m}^{-3}$, and $N_o = 10^{14}\,\text{m}^{-3}$ ($\nu = 10\,\text{MHz}$, $\theta_o = 30°$, and

$\phi = 90°$. Fig. 7a shows that the reflected power increases with increasing the central density. Fig. 7b shows that the transmitted power decreases with the central density, while the absorbed power increases with increasing the density, as shown in Fig. 7c.

These behaviors are expected, since increasing the electron density forces the plasma to behave like a perfect conductor. It is clear from Fig. 7 that the resonance frequency increases with increasing the central density. Physically, this can be explained as a frequency scaling phenomenon, since for a slab of finite volume, increasing the electron density results in decreasing the average distance between the particles which can be compensated by decreasing the wave length, i.e., increasing the frequency, of the interacting electromagnetic wave.

From the behavior of the three types of power, one can deduce the appropriate parameters for the plasma slab to operate as reflector, transmitter, or absorber via varying the plasma parameters, e.g., ν and N_o. For example, the reflected power is small if the plasma has high collision frequency and low density number. The two requirements, namely, low density and high collision frequency, seem hard to achieve simultaneously. The weakly ionized but turbulent plasma generated by Penning discharges achieve such conditions [5]. Binary collisions are not dominant in these plasmas, but rather effective collisions which transfer momentum between the turbulent waves and the particles.

4. CONCLUSION

In order to study the EM waves interaction with a plasma slab, SMM was developed and verified. SMM is found to be a numerically efficient tool from the computation time and storage point of view. Reflection, transmission, and absorption of electromagnetic waves from nonuniform magnetized plasma slab are studied. The effects of varying the wave frequency as well as the plasma parameters on reflected, transmitted, and absorbed power are presented and discussed. Referring to the numerical results, it is found that the main function of the plasma slab has been greatly dependent on the wave frequency. The degree of reflection and transmission has found to be affected by the plasma parameters.

This study finds a lot of applications such as the diagnosis of the plasma without disturbing it. Conventional diagnostic devices, such as probes for measuring electrostatic and magnetic fields, not only contaminate the plasma but are often too large for the investigation of the microscopic structure of the plasma. The most efficient way for the diagnosis process is the electromagnetic wave scattering by the plasma body under investigation.

REFERENCES

1. Helaly, A., E. A. Soliman, and A. A. Megahed, "An analytic method for dealing with ionosphere propagation," *Proceedings of ANTEM'96 Conf.*, Montréal, Québec, Canada, 1996.

2. Vidmar, R. J., "On the use of atmospheric plasmas as electromagnetic reflectors and absorbers," *IEEE Trans. on Plasma Science*, Vol. 18, 733-741, 1990.

3. Destler, W. W., J. E. Degrange, H. H. Fleischmann, J. Rodgers, and Z. Segalov, "Experimental studies of high power microwave reflection, transmission, and absorption from a plasma-covered plane boundary," *J. Appl. Phys.*, Vol. 69, No. 9, 6313–6318, 1991.

4. Bittencourt, J. A., *Fundamentals of Plasma Physics*, Pergamon Press, Oxford, 1986.

5. Laroussi, M. and J. R. Roth, "Numerical calculation of the reflection, absorption, and transmission of microwaves by a nonuniform plasma slab," *IEEE Trans. on Plasma Science*, Vol. 21, No. 4, 366–372, Aug. 1993.

6. Gilbert, F. and G. E. Backus, "Propagator matrices in elastic wave and vibration problems," *Geophys.*, Vol. 31, 326–332, 1966.

7. Morgan, M. A., D. L. Fisher, and E. A. Milne, "Electromagnetic scattering by stratified inhomogeneous anisotropic media," *IEEE Trans. Antennas Propagat.*, Vol. AP-35, 191–197, 1987.

8. Titchener, J. B. and J. R. Willis, "The reflection of electromagnetic waves from stratified anisotropic media," *IEEE Trans. Antennas Propagat.*, Vol. AP-39, 35–39, Jan. 1991.

9. Gray, K. G., "An exact solution for the impulse response of uniform plasma half space," *IEEE Trans. Antennas Propagat.*, Vol. AP-22, 819–821, Nov. 1974.

10. Zhang, D. Y. and K. K. Tschu, "Propagation of electromagnetic pulse with a Gaussian envelope through an inhomogeneous anisotropic plasma layer," *Radio Sci.*, Vol. 22, 635–642, July/Aug. 1987.

11. Lee, J. J., "Pulse distortion through a lossy plasma medium," *IEEE Trans. Antennas Propagat.*, Vol. AP-27, 880–885, Nov. 1979.

12. Whitman, G. M. and L. B. Felsen, "FM pulses in stratified isotropic plasma," *IEEE Trans. Antennas Propagat.*, Vol. AP-27, 596–603, Sept. 1979.

13. Hagelaar, G. J. M., K. Hassouni, and A. Gicquel, *Journal of Applied Physics*, Vol. 96, 1819, 2004.

14. Hojo, H., A. Fukuchi, A. Itakura, and A. Mase, *Review of Scientific Instruments*, Vol. 75, 3813, 2004.

15. Kunz, K. S. and R. J. Luebbers, *The Finite Difference Time Domain Method for Electromagnetics*, CRC Press, Inc., Florida, 1993.

16. Helaly, A., E. A. Soliman, and A. A. Megahed, "Electromagnetic waves scattering by nonuniform plasma cylinder," *IEE Proc. - Microw. Antennas Propag.*, Vol. 144, No. 2, 61–66, April 1997.

17. Helaly, A., E. A. Soliman, and A. A. Megahed, "Electromagnetic waves scattering by nonuniform plasma sphere," *Canadian Journal of Physics*, Vol. 75, 919–932, 1997.

18. Kodis, R. D., "Propagation and scattering in plasmas," *Proc. IEEE*, Vol. 53, 1016–1024, 1965.

19. Heald, M. A. and C. B. Wharton, *Plasma Diagnostics with Microwaves*, Wiley and Sons Inc., New York, 1965.